Desalination and Water Treatment
www.deswater.com
doi: 10.1080/19443994.2014.931525

53 (2015) 2760–2766
March

Influence of divalent cations adsorption on the performance of electromembrane process

Hong-Joo Lee[a,*], Mun-Kyung Hong[b], Seung-Hyeon Moon[c]

[a]*Department of Bioenergy Science and Technology, Chonnam National University, 77 Yongbong-ro, Buk-gu, Gwangju 500 757, Korea, Tel. +82 62 530 2040; email: hjlee68@jnu.ac.kr*
[b]*Department of Environmental Research and Analysis, Korea Environment Corporation, Environmental Research Complex, Kyungseo-dong, Seo-gu, Incheon 404 708, Korea*
[c]*School of Environmental Science and Engineering, Gwangju Institute of Science and Technology (GIST), 261 Cheomdangwagi-ro, Buk-gu, Gwangju 500 712, Korea*

Received 16 July 2013; Accepted 25 November 2013

ABSTRACT

In this study, the adsorption equilibrium and kinetics of divalent cations were studied to describe transport phenomena occurring in an electromembrane process. The adsorption isotherms of divalent cations over cation-exchange resins were fitted to the Langmuir and Freundlich isotherms. Adsorption equilibrium experiments of divalent cations showed the preferential adsorption between adsorbent and adsorbate and Ca^{2+} showed about five times higher adsorption capacity than Mg^{2+}. Adsorption kinetics was studied using the reversible first-order model and the forward and reverse reaction rate constants were estimated for divalent cations adsorption. The forward reaction rate constants for the removal of divalent cations were much higher than the reverse reaction rate constants, indicating that the rate of adsorption was dominant in ion-exchange process. In this study, the higher removal efficiency of Ca^{2+} than Mg^{2+} in an electromembrane process could be understood by the adsorption equilibrium and kinetic study.

Keywords: Adsorption; Divalent cations; Electromembrane process; Ion exchange

1. Introduction

Hardness ions represent the contents of cations such as iron, manganese, calcium, and magnesium in water. They are responsible for the formation of deposits and degradation of soap by the reaction with soap anions or precipitation in forms of sulfates or carbonates in many effluents [1–3]. Among hardness ions, calcium (Ca^{2+}) and magnesium (Mg^{2+}) are known as dominant species.

Various methods have been widely applied as a means of effective water softening to remove divalent ions, as follows: chemical precipitation, ion-exchange process, nanofiltration, reverse osmosis, and electromembrane process [4,5]. In case of the chemical precipitation, the choices of additional chemicals are restricted for the purpose of drinking water [6–8]. Among water softening processes, ion exchange has

---

*Corresponding author.

Presented at 2013 International Environmental Engineering Conference and Annual Meeting of the Korean Society of Environmental Engineers (IEEC 2013) Seoul, Korea, June 11–13, 2013

been broadly used due to ease of operation and high-removal efficiency [9,10]. However, high concentration of monovalent cations releases during the ion-exchange process, which may result in harmful effects on environments and the periodical regeneration of resins requires when the ion-exchange capacity becomes saturated. Therefore, a cost effective and low energy consuming electrochemical method has been forced on water softening process. Among water softening processes, electromembrane processes such as electrodialysis and electrodeionization have been studied as an alternative of ion-exchange process.

Electrodeionization, an electromembrane process combining electrodialysis and ion-exchange process, has been considered one of the potential methods for removing hardness materials without periodic regeneration of resins [11,12]. Like electrodialysis, anion- and cation-exchange membranes are arranged in alternating series with compartments forming between the cathode and anode and packed ion-exchange resins. A feed solution is pumped through the dilute compartment and an electrical potential is applied between two electrodes, then positively charged cations migrate toward the cathode and anions toward the anode. The overall result is an increase in ion concentration in alternate compartments and the simultaneous depletion of ions in dilute compartment [12–14].

In the previous studies, electrodeionization showed the high transport rate and the removal efficiency of Ca^{2+} was higher than that of Mg^{2+}. The results can be understood by the different sorption equilibrium and kinetics of cations [15–17]. The objective of this study is to investigate the adsorption equilibrium and kinetics of divalent cations occurring on ion-exchange resins and to describe transport phenomena in electromembrane processes. In this study, the adsorption equilibriums (Freundlich and Langmuir sorption isotherms) were considered using the relationship between adsorbed amount on the adsorbent and the concentration in the fluid. In addition, kinetics of adsorption describing the solute uptake rate was studied as one of the important characteristics defining the efficiency of sorption.

2. Experimental

In this study, Amberlite IR 120Na (Rohm and Hass Co., USA) was used as cation-exchange resin. The resin has a polymeric matrix of Styrene DVB copolymer with functional group of $–SO_3^-$ and the total exchange capacity of above 2.0 meq/mg [3]. The dried material at 105˚C was used for further experimental works. For the adsorption equilibrium studies, cation-exchange resin was taken in different glass bottle containing different concentrations of divalent cations. The bottles were stirred thoroughly in a temperature-controlled shaker for 24 h at room temperature. During the equilibrium experiment, stirring speed set to 70 rpm and 20˚C. Solution was sampled periodically for the divalent cation analysis.

In addition, kinetic study was conducted at 20˚C in a well-mixed glass bottle with a cover. The stirring speed was at 70 rpm to maintain resin particles in suspension. Solution containing 10–200 mg/L of divalent cations (Ca^{2+} and Mg^{2+}) was prepared using stock solutions of Ca(II) chloride, Mg(II) sulfate prepared with Milli-Q water (18 MΩ). All reagents used in this study were of analytical reagent grade. The prepared feed solution was injected into the unit cell by a Cole-Parmer Masterflex® pump (Barrington, IL).

Ionic species were analyzed using the ion chromatography (DX-120, DIONEX, USA) with AS40 autosampler and a standard conductivity cell. Cation-exchange CS12A column with a guard column CG-12 was used to measure Ca^{2+} and Mg^{2+}. Eluent was prepared with 18 mM methanesulfonic acid and pumped at the flow rate of 1.0 ml/min.

3. Results and discussion

3.1. Adsorption isotherm

In general, adsorption isotherm experiments are usually done to measure the effectiveness of adsorption for removing specific adsorbates as well as to determine the maximum adsorption capacity [18,19]. Several models have been used in the literature to describe the experimental data of adsorption isotherms. The Langmuir and Freundlich models are the most frequently employed ones [20–22].

Fig. 1 shows the adsorption isotherm of divalent cations on the cation-exchange resin (Amberlite IR120) in the solution containing different concentrations (10–200 mg/L) of Ca^{2+} and Mg^{2+} at 20˚C. In the adsorption isotherm, divalent cations adsorption increased with increasing concentration of the adsorbate. In addition, the adsorption of Ca^{2+} was higher than that of Mg^{2+} shown in the figure.

In this study, the Langmuir and Freundlich adsorption isotherms were considered to describe ion-exchange behaviors of divalents on cation-exchange resins. Of adsorption isotherms, the Langmuir isotherm model is valid for monolayer adsorption on to the surface containing finite number of identical sorption sites. The Langmuir equation relates solid-phase adsorbate concentration (q_e) to the equilibrium liquid

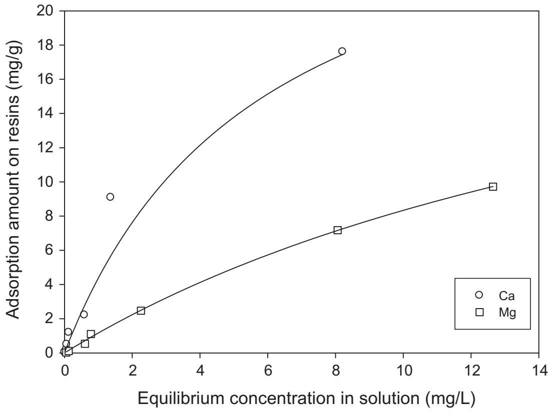

Fig. 1. Adsorption of Ca and Mg on the cation-exchange resin.

concentration (C_e). In order to explain the adsorption mechanism of Ca and Mg over cation-exchange resins, the data were fitted to the Langmuir model i.e.,

$$q_e = \frac{Q_0\, bC_e}{1 + bC_e} \tag{1}$$

where Q_0 (mg/g) is the maximum amount of adsorbate per unit weight of adsorbent to form a complete monolayer on the surface and b the Langmuir constant (L/mg) related to the affinity of the adsorption sites. The equation can be rearranged to linear form for determining the Langmuir constants as follows:

$$\frac{1}{q_e} = \frac{1}{Q_0 b}\frac{1}{C_e} + \frac{1}{Q_0} \tag{2}$$

Fig. 2 shows the linear relationship between $1/q_e$ and $1/C_e$ for various initial concentrations using Eq. (2), indicating the applicability of the classical adsorption isotherm to this adsorbate–adsorbent system.

The Freundlich sorption isotherm is empirical equation based on sorption on heterogeneous surface, which is expressed as follows:

$$q_e = K_F {C_e}^n \tag{3}$$

where K_F and n are coefficient, q_e and C_e are the weight adsorbed per unit weight of adsorbent and adsorbate concentration at equilibrium, respectively. The relation between q_e and C_e is given by:

$$\ln q_e = n \ln C_e + \ln K_F \tag{4}$$

where the intercept, $\ln K_F$, is a measure of adsorbent capacity and the slope $(1/n)$ is the sorption intensity [19]. In the Freundlich isotherm of Ca^{2+} and Mg^{2+} shown in Fig. 3, the plot of $\ln q_e$ and $\ln C_e$ for various initial concentrations showed linear relationship and the coefficients K_F and n were estimated using Eq. (4).

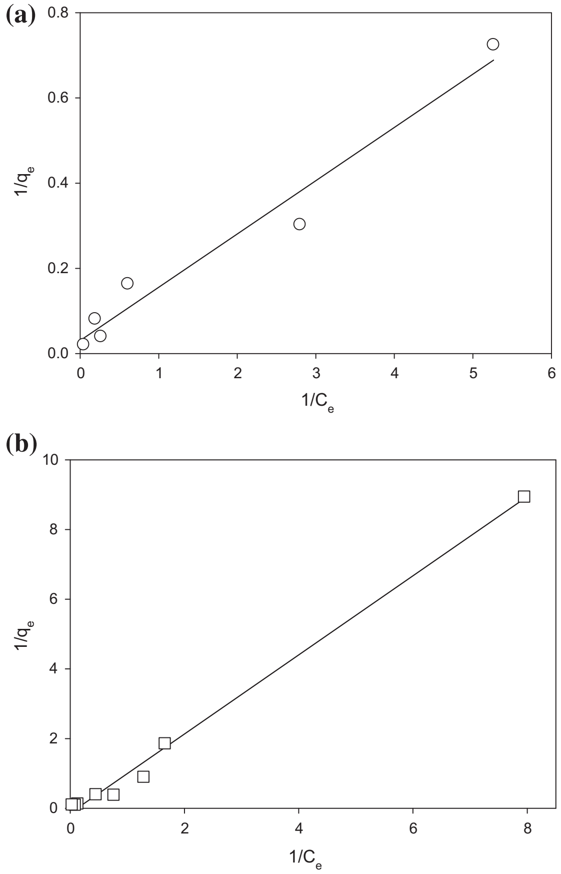

Fig. 2. Langmuir isotherm of Ca (a) and Mg (b).

Table 1 shows the values of adsorption isotherms with correlation coefficient (r^2). In the Langmuir isotherm of Ca^{2+} and Mg^{2+} over cation-exchange resins, the values of Q_0 and b was estimated to 32.36 mg/g and 0.24 L/mg for Ca^{2+}, much higher value than Mg^{2+} (7.23 mg/g and 0.12 L/mg). In addition, the adsorption capacity of Ca^{2+} in the Freundlich isotherm were found to be 5.43 mg/g, about five times than that of Mg^{2+} (1.19 mg/g). The higher value for K_F indicates the higher affinity during the adsorption of ion-exchange resin. Also, the adsorption intensities (n) of Ca^{2+} and Mg^{2+} were found 0.87 and 0.95, respectively, implying the preferential adsorption between adsorbent and adsorbate [19]. From the result, the adsorption capacity of Ca^{2+} was observed to be much higher than that of Mg^{2+}, suggesting that that the removal efficiency of Ca would be higher than Mg^{2+} in ion-exchange process.

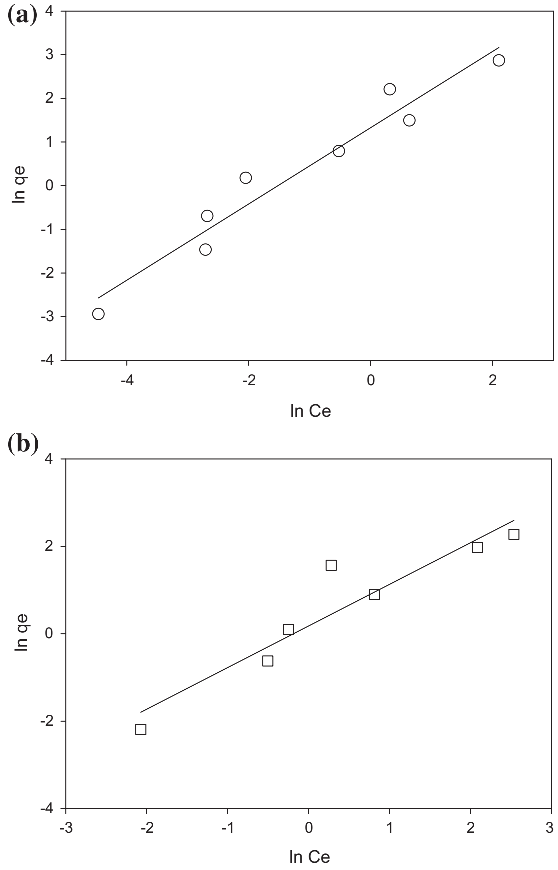

Fig. 3. Freundlich isotherm of Ca (a) and Mg (b).

3.2. Adsorption kinetics

When any single species adsorbs on the heterogeneous surface, the adsorption of the adsorbate from aqueous solution follows the reversible first-order kinetics, when a single species is considered on a heterogeneous surface [22,23]. Kinetics of sorption describing the solute uptake rate is one of the important characteristics defining the efficiency of sorption. The sorption of ions from liquid phase to solid phase is expressed as:

$$A \underset{k_2}{\overset{k_1}{\longleftrightarrow}} B \tag{5}$$

where k_1 and k_2 are the rate constants for the forward and reverse direction reaction, respectively. The adsorption rate can be expressed as follows:

$$\frac{dx}{dt} = k_1(a - x) - k_2 x \tag{6}$$

where a is the initial concentration of ions, x the amount transferred from liquid phase to solid phase at any time t. The equilibrium constant, K_C, can be expressed using the concentration at equilibrium, X_e, as follows:

$$K_C = \frac{X_e}{a - X_e} = \frac{k_1}{k_2} \tag{7}$$

Eq. (6) can be rewritten as follows:

$$k_1 + k_2 = \frac{1}{t}\ln\frac{X_e}{X_e - x} \tag{8}$$

$$-\ln\left(1 - \frac{x}{X_e}\right) = (k_1 + k_2)t \tag{9}$$

Eq. (9) can be written using a fractional attainment of equilibrium of ions (U_t) and the overall rate constant (k) as follows:

$$\ln\,(1 - U_t) = -(k_1 + k_2)t = -kt \tag{10}$$

$$k = k_1 + k_2 = k_1 + \frac{k_1}{K_C} = k_1\left(1 + \frac{1}{K_C}\right) \tag{11}$$

where U_t is defined as:

Table 1
Langmuir and Freundlich Isotherms of divalent cations over the Amberlite IR 120 resins

	Langmuir isotherm			Freundlich isotherm		
	Q_0 (mg/g)	b (L/mg)	Correlation coefficient	K_F (mg/g)	n	Correlation coefficient
Ca^{2+}	32.36	0.24	0.965	5.43	0.87	0.929
Mg^{2+}	7.23	0.12	0.993	1.19	0.95	0.889

$$U_t = \frac{x}{X_e} = \frac{C_{A(0)} - C_{A(t)}}{C_{A(0)} - C_{A(e)}} \tag{12}$$

where $C_{A(0)}$ is the initial concentration of ion, $C_{A(t)}$ is the concentration of ions present at any time (t), and $C_{A(e)}$ is the concentration of ions present at equilibrium condition.

The adsorption kinetic experiments were performed in the divalent cation concentration range of 10–200 mg/L. The equilibrated concentration of Ca^{2+} and Mg^{2+} was plotted as a function of the contact time as shown in Fig. 4. The concentration of Ca^{2+} and Mg^{2+} decreased rapidly within initial 5–6 h and then, the adsorption is virtually completed after 6–8 h.

Using the kinetic equations, the overall reaction rate constant, the forward and reverse reaction rate constants for a given concentration were calculated from the plot $\ln(1 - U_t)$ vs. time as shown in Fig. 5. Table 2 shows the rate constants for divalent cations adsorption using the reversible first-order model. The results showed that the forward rate constants for the removal of divalent cations were much higher than the reverse rate constants for the desorption process [22]. The results imply that the rate of adsorption is clearly dominant and the desorption hardly takes place in the ion-exchange process.

The rate constants of Ca^{2+} increased with increasing its concentration, whereas in Table 2 they showed opposite for Mg^{2+}, which is related to selectivity and diffusion coefficient of divalent cations on the ion-exchange resin. The selectivity can affect the boundary condition at the surface of the particle resins, which depends on the nature of the ion exchange and the concentration of solutions. The counter ion with higher adsorption capacity is taken up at a faster rate and releases at a slow rate [24]. Calcium ion, which has much higher preference or selectivity as presented in Table 1, showed increasing forward reaction rate and decreasing reverse reaction rate with increasing concentration. In

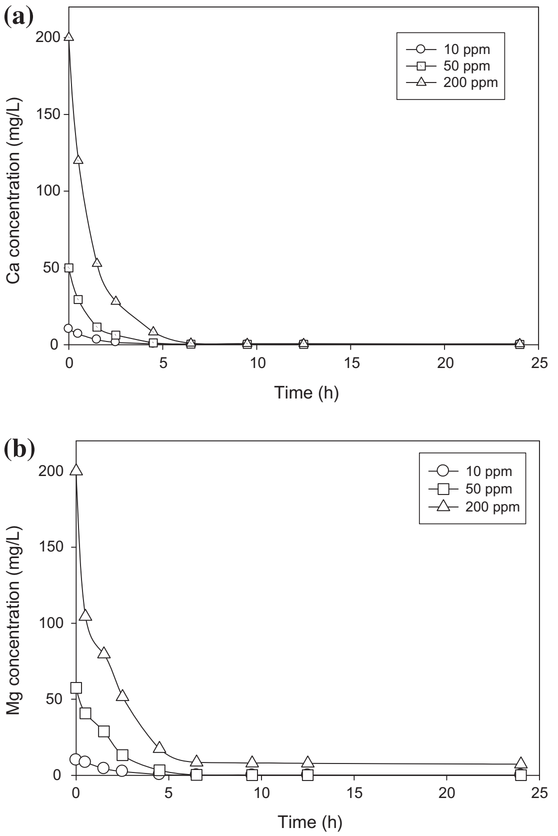

Fig. 4. Adsorption of Ca (a) and Mg (b) on Amberlite IR120 with time.

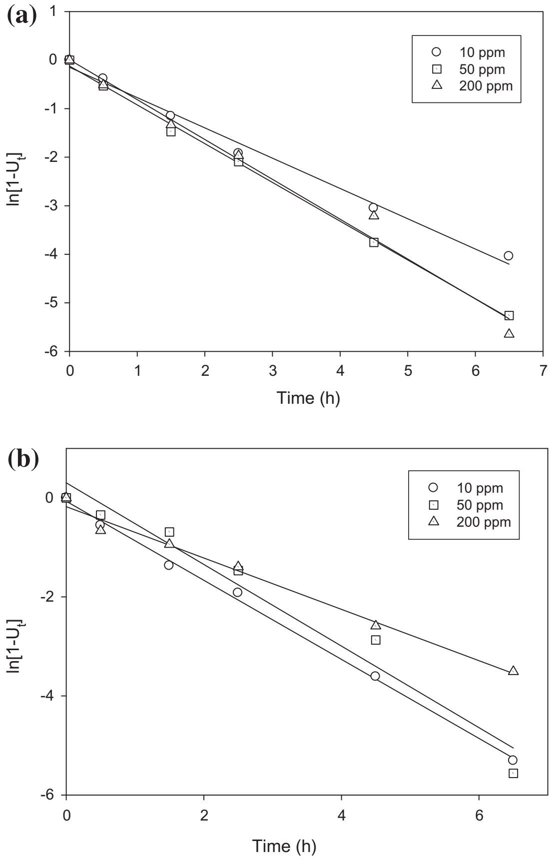

Fig. 5. Adsorption kinetics fitted to the reversible first-order model of Ca (a) and Mg (b).

Table 2
Reaction rate constant for the removal of Mg and Ca with Amberlite IR 120

	Concentration (mg/L)	Overall rate constant $k = k_1 + k_2$ (h^{-1})	Forward reaction rate constant k_1 (h^{-1})	Reverse reaction rate constant k_2 (h^{-1})
Mg^{2+}	10	0.7983	0.7938	0.0045
	50	0.8239	0.8202	0.0037
	200	0.5187	0.4965	0.0221
Ca^{2+}	10	0.6414	0.6271	0.0143
	50	0.8254	0.8202	0.0051
	200	0.8764	0.8725	0.0039

Table 3
Removal of divalent cations in the electrodeionization reversal systems

Flow rate[a] (ml/min)	Removal of Ca^{2+} (%)	Removal of Mg^{2+} (%)
30	99.8	99.9
100	98.8	97.8
200	98.6	98.8
300	95.6	93.3
400	94.5	92.4
500	93.4	92.1

[a] Experimental condition: 20 V of electrical potential, 250 mg/L as $CaCO_3$ of hardness concentration, 20 min of the polarity reversal time [3].

addition, the overall rate constant of the ion-exchange process can be correlated to the pore diffusion coefficient and film diffusion coefficient. Based on the estimated results, film diffusion is the rate-determining step in the cation adsorption on ion-exchange resin and overall diffusion coefficient showed similar trend with different chromium concentrations [22].

3.3. Relationship between divalent adsorption and the removal of divalent cations

The removal efficiencies of divalent cations on the electrodeionization reversal with periodical polarity change were considered to investigate the influence of adsorption on the removal of divalent cations. The previous study was performed at the different flow rates and hardness concentrations [3]. Table 3 shows the influence of flow rate on the divalent cation removal efficiencies. As the flow rate increased, the removal efficiencies decreased due to shorter contact time. As shown in the table, the removal efficiencies were similar at low flow rates. However, Ca^{2+} showed higher values than Mg^{2+} at higher flow rates.

Ca^{2+} showed about five times higher adsorption capacity than Mg^{2+} in Table 1. Nevertheless, the removal efficiency of Ca^{2+} showed higher value within 1–2%, which could be understood by that the removal efficiency is affected by many parameters process characteristics, operational mode, as well as adsorption capacity.

In addition, the electrodeionization reversal results on the hardness concentration showed that Ca^{2+} showed higher removal efficiency. At the electrodeionization reversal experiment of high hardness concentration (630 mg/L as $CaCO_3$), the removal of Ca^{2+} was 84.5%, while that of Mg^{2+} was 81.3%. Through the study, the results of adsorption equilibrium and kinetic study could explain the higher removal efficiency of Ca^{2+} in the electrodeionization process.

4. Concluding remarks

In this study, the adsorption equilibrium and kinetics were studied to describe transport phenomena occurring in an electrodeionization process. The adsorption isotherms of Ca^{2+} and Mg^{2+} over the cation-exchange resin (Amberlite IR120) showed that adsorption amount of Ca^{2+} was higher than that of Mg^{2+}. Data obtained in the adsorption equilibrium experiments were fitted well to the Langmuir and Freundlich isotherms and the estimated values related to adsorption capacity of Ca^{2+} were five times higher than that of Mg^{2+}. The adsorption kinetic study results showed that the forward reaction rate constants for the removal of divalent cations were much higher than the reverse reaction rate constants related to the desorption process. The results showed that the rate of adsorption is clearly dominant and the desorption hardly takes place in ion-exchange process.

The removal efficiency of Ca^{2+} showed higher value within 1–2% in the electrodeionization reversal even though Ca^{2+} showed higher adsorption capacity than Mg^{2+}, implying that the removal efficiency is affected by many process parameters as well as adsorption capacity. The study on the adsorption equilibrium and kinetics could explain the higher removal efficiency of Ca^{2+} in the electromembrane process.

References

[1] J.S. Park, J.H. Song, K.H. Yeon, S.H. Moon, Removal of hardness ions from tap water using electromembrane processes, Desalination 202 (2007) 1–8.

[2] J.H. Kweon, D.F. Lawler, Fouling mechanisms in the integrated system with softening and ultrafiltration, Water Res. 38 (2004) 4164–4172.

[3] H.J. Lee, M.K. Hong, S.H. Moon, A feasibility study on water softening by electrodeionization with the periodic polarity change, Desalination 284 (2012) 221–227.

[4] B. van der Bruggen, C. Vandecateele, Removal of pollutants from surface water and groundwater by nanofiltration: Overview of possible applications in the drinking water industry, Environ. Pollut. 122 (2003) 435–445.

[5] E. Yildiz, A. Nuhoglu, B. Keskinler, G. Akay, B. Farizoglu, Water softening in a crossflow membrane reactor, Desalination 159 (2003) 139–152.

[6] S.J. Seo, H. Jeon, J.K. Lee, G.Y. Kim, D. Park, H. Nojima, J. Lee, S.H. Moon, Investigation on removal of hardness ions by capacitive deionization (CDI) for water softening applications, Water Res. 44 (2010) 2267–2275.

[7] C. Gabrielli, G. Maurin, H. Francy-Chausson, P. Thery, T.T.M. Tran, M. Tlili, Electrochemical water softening: Principle and application, Desalination 201 (2006) 150–163.

[8] S. Ghizellaoui, A. Chibani, S. Ghizellaoui, Use of nanofiltration for partial softening of very hard water, Desalination 179 (2005) 315–322.

[9] Z. Yu, T. Qi, J. Qu, L. Wang, J. Chu, Removal of Ca(II) and Mg(II) from potassium chromate solution on Amberlite IRC 748 synthetic resin by ion exchange, J. Hazard. Mater. 167 (2009) 406–412.

[10] A.A. Hekmatzadeh, A. Karimi-Jashni, N. Talebbeydokhti, B. Kløve, Adsorption kinetics of nitrate ions on ion exchange resin, Desalination 326 (2013) 125–134.

[11] A. Grabowski, G. Zhang, H. Strathmann, G. Eigenberger, The production of high purity water by continuous electrodeionization with bipolar membranes: Influence of the anion-exchange membrane permselectivity, J. Membr. Sci. 281 (2006) 297–306.

[12] H. Strathmann, Electrodialysis, a mature technology with a multitude of new applications, Desalination 264 (2010) 268–288.

[13] J.H. Song, K.H. Yeon, S.H. Moon, Effect of current density on ionic transport and water dissociation phenomena in a continuous electrodeionization (CEDI), J. Membr. Sci. 291 (2007) 165–171.

[14] J. Wood, J. Gifford, J. Arba, M. Shaw, Production of ultrapure water by continuous electrodeionization, Desalination 250 (2010) 973–976.

[15] H.J. Lee, J.H. Song, S.H. Moon, Comparison of electrodialysis reversal (EDR) and electrodeionization reversal (EDIR) for water softening, Desalination 314 (2013) 43–49.

[16] E. Pehlivan, T. Altun, The study of various parameters affecting the ion exchange of Cu^{2+}, Zn^{2+}, Ni^{2+}, Cd^{2+}, and Pb^{2+} from aqueous solution on Dowex 50W synthetic resin, J. Hazard. Mater. 134 (2006) 149–156.

[17] A. Demirbas, E. Pehlivan, F. Gode, T. Altun, G. Arslan, Adsorption of Cu(II), Zn(II), Ni(II), Pb(II), and Cd(II) from aqueous solution on Amberlite IR-120 synthetic resin, J. Colloid Interface Sci. 282 (2005) 20–25.

[18] S. Singh, V.C. Srivastava, I.D. Mall, Fixed-bed study for adsorptive removal of furfural by activated carbon, Colloids Surf. A 332 (2009) 50–56.

[19] C.P. Dwivedi, J.N. Sahu, C.R. Mohanty, B.R. Mohan, B.C. Meikap, Column performance of granular activated carbon packed bed for Pb(II) removal, J. Hazard. Mater. 156 (2008) 596–603.

[20] Z. Chen, W. Ma, M. Han, Biosorption of nickel and copper onto treated alga (*Undaria pinnatifida*): Application of isotherm and kinetic models, J. Hazard. Mater. 155 (2008) 327–333.

[21] B.H. Hameed, M.I. EI-Khaiary, Sorption kinetics and isotherm studies of a cationic dye using agricultural waste: Broad bean peels, J. Hazard. Mater. 154 (2008) 639–648.

[22] S. Rengaraj, K.H. Yeon, S.H. Moon, Removal of chromium from water and wastewater by ion exchange resins, J. Hazard. Mater. 87 (2001) 273–287.

[23] S.N. Milmile, J.V. Pande, S. Karmakar, A. Bansiwal, T. Chakrabarti, R.B. Biniwale, Equilibrium isotherm and kinetic modeling of the adsorption of nitrates by anion exchange Indion NSSR resin, Desalination 276 (2011) 38–44.

[24] F. Helfferich, Ion Exchange, McGraw-Hill, New York, NY, 1962, pp. 95–249.